



New routes for complete regeneration of coked zeolite

L.Y. Jia^a, Al Farouha^b, L. Pinard^{b,*}, S. Hedan^b, J.-D. Comparot^b, A. Dufour^a, K. Ben Tayeb^c, H. Vezin^c, C. Batiot-Dupeyrat^{b,*}

^a LRGP, CNRS, Université de Lorraine, 1 rue Grandville, 54000 Nancy, France

^b Université de Poitiers, CNRS UMR7285, Institut de Chimie des Milieux et Matériaux de Poitiers, B27, TSA 51106, 4 rue Michel Brunet, 86073 Poitiers CEDEX 9, France

^c Université de Lille, Sciences et Technologies, LASIR Bât. C4 – Bureau 006 59655 Villeneuve d'Ascq, France

ARTICLE INFO

Article history:

Received 23 May 2017

Accepted 15 July 2017

Available online 19 July 2017

Keywords:

Zeolite

Non-thermal plasma

Coke

EPR

Radical

ABSTRACT

Among alternative techniques to overcome the difficulties associated with thermal regeneration of coked zeolite, non-thermal plasma can be considered as one of the most promising technology. A complete regeneration of zeolite can be achieved at room temperature with a low energy consumption. The active species responsible for catalyst regeneration are the short-lived oxygenated species and not ozone. Based on EPR analysis, which allows the mapping of radicals, the active species generated by NTP are able to diffuse within zeolite eliminating coke molecules. The efficiency of regeneration is directly related to the number of active species present in gas phase. A simple way to increase their concentration consists to substitute N₂ by a noble gas as He. In this case, coke is totally oxidized into CO₂, 6 times faster than under air.

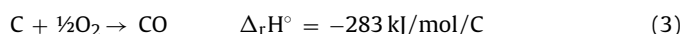
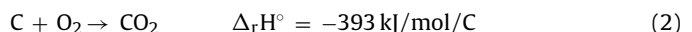
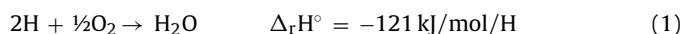
© 2017 Elsevier B.V. All rights reserved.

1. Introduction

Catalyst deactivation, is a problem of great and continuing concern in industrial catalytic processes. The cost to industry for catalyst replacement and/or regeneration is estimated at several billions of dollars per year [1]. The question that determines the future of the deactivated catalyst, i.e. rejuvenation, regeneration or in the worst-case its replacement, is related to the reversibility of deactivation [2]. Deactivation caused by poisoning, fouling and deposition of heavy compounds is generally reversible, and therefore regeneration is possible, while in the case of chemical transformation, thermal or mechanical degradations, deactivation is irreversible [3]. Poisoning by strong chemisorption of reactants or products and coke formation by cracking/condensation reactions are the main sources of catalyst deactivation. The chemical composition of coke depends largely on the nature of catalyst, the feed composition and the operating conditions especially temperature. The coke can be either graphitic or polyaromatic molecules more or less alkylated, and even functionalized [4,5]. The usual treatment for its removal is combustion in air [2], such as in fluid catalytic

cracking where coke is oxidized in a fluidized bed operating continuously.

The coke combustion forms initially water then CO₂ or CO [6]. The high exothermicity of combustion reactions (Eqs. (1)–(3)) and the limited thermal stability of most catalysts make difficult the control of the process temperature. Hot spots can appear (especially, where the coke is located) leading to irreversible damages i.e. metal sintering, zeolite dealumination....



To avoid a thermal runaway, a first solution consists in carrying out the combustion of coke in a fluidized bed reactor in two successive stages; the first stage being maintained at a low temperature just enough to burn hydrogen atoms and a part of carbon atoms, while the second stage is maintained at a higher temperature to remove the more stable residual coke. This procedure is commonly used in fluid catalytic cracking process (FCC) [7,8]. Conventional operating conditions of a regenerator are: 950 < T < 1050 K and residence time between 5 and 10 min [2]. Another solution to limit the oxidation temperature and the regeneration time is to add a very small amount of noble metal (1 ppm Pt by example) to the coking catalyst, thereby ensuring complete combustion at lower temperature and minimizing the afterburning. Despite

* Corresponding authors.

E-mail addresses: ludovic.pinard@univ-poitiers.fr (L. Pinard), catherine.batiot.dupeyrat@univ-poitiers.fr (C. Batiot-Dupeyrat).

these improvements, zeolite modification (dealumination) during regeneration process is still an unresolved problem and part of deactivated catalyst must be replaced by fresh catalyst. In a FCC unit, the amount of catalyst used reaches 100–300 tons every 2 months [2]. Consequently, to limit the cost associated with catalyst replacement, the development of efficient and milder regeneration methods is of particular interest.

More expensive oxidizing agents such as ozone was used to remove coke from zeolites. With ozone-enriched oxygen, coke can be oxidized at a temperature lower than 523 K without risk of hydrothermal degradation. However, the use of this strong oxidant is limited because coke located in the core of extrudates cannot be removed due to the rapid dissociation of O₃ [8]. The half-life time of ozone in air at 523 K is only 1.5 s and is much more lower in the presence of heterogeneous catalyst. Moreover, the use of ozone in industrial processes should be avoided since ozone emission into the atmosphere is strictly controlled and could not exceed 75 ppb. N₂O is also a potential oxidizing agent, it is moreover cheaper than O₃ and is even produced as waste in adipic acid preparation. However, relatively high temperatures (700–800 K) are required for coke removal by nitrous oxide. Consequently, despite the interesting results obtained [9], the substitution of classical combustion processes under air by N₂O treatment seems very unlikely.

Among alternative techniques to overcome the difficulties associated with thermal regeneration, non-thermal plasma can be considered as a promising technology due to its non-equilibrium characteristics [10]. In such a plasma, highly energetic electrons are generated at atmospheric pressure and low temperature (room temperature), it leads to the formation of highly active species such as radicals, excited atoms, ions and molecules. The generated reactive species play important roles in the initiation and propagation of many physical and chemical reactions [11]. Under oxygen plasma, the most abundant species formed are the positive ion O₂⁺, the negative ions O⁻, O₂⁻ and O₃ [12]. Bibby et al. [13] reported for the first time in 1986 that Radio-Frequency oxygen plasma can be used to remove coke from the surface of ZSM-5 zeolite while the authors observed that internal coke was not eliminated. Khan et al. [14] showed that O-atoms obtained by O₂ dissociation in a glow discharge plasma can lead to the partial decoking of a zeolite. However, such a plasma can only be generated at pressures of the order of 10⁻³ mbar, which make the process little attractive for industrial applications. A dielectric barrier discharge (DBD) reactor operating at atmospheric pressure was used by Hafezkhiaibani et al. [15] to perform the decoking of Pt-Sn/Al₂O₃ catalyst. A complete carbon removal was obtained using argon as diluent gas with oxygen, but the structural properties of the catalyst was modified after the regeneration step: decrease of surface area and metal dispersion.

Consequently, there are needs to perform complementary studies on the use of non-thermal plasma for coke removal.

In this study, a Dielectric Barrier Discharge (DBD) plasma reactor with a pin to plate geometry was used. The coked zeolite was shaped as a wafer and placed into the discharge zone. The influence of the nature of gas (air or He + O₂), deposited power and treatment duration was investigated. Coke removal was determined using the classical method ATD-ATG, the textural and structural properties of zeolite were characterized after plasma treatment by surface area measurement, IR analysis (acidity). Moreover, it was possible to evaluate the efficiency of plasma treatment at the surface of the wafer using a CMOS camera and after image treatment by shades of grey.

Since some coke molecules, trapped in the pores of zeolite, can lead to the formation of radicals by spontaneous ionization [16], the 2D-EPR spectroscopy was used to determine the localization of radicals in the disk [17]. This analytical technic is an interesting tool to understand how coke elimination occurs under the plasma

Table 1
Characterizations of fresh and coked zeolites.

	Unit	Fresh	Coked
Coke ^a	wt.%	0	6.5
Soluble coke	—	—	2.6
Insoluble coke	—	—	3.9
V _{micro} ^b	cm ³ /g	0.15	0.10
V _{meso} ^c	—	0.38	0.39
[PyH ⁺] ^d	μmol/g	242	158
[PyL] ^e	—	63	38

^aMeasured by ATD/ATG; ^bMicropore volume obtained by using t-plot method;

^cmesopore volume = V_{total} – V_{micro} (V_{total} determined from the adsorbed volume at p/p₀ = 0.99); ^{d,e}measured by pyridine adsorbed on Brønsted and Lewis acid sites after evacuation at 423 K.

discharge. To the best of our knowledge, such study has never been reported before.

2. Experimental part

2.1. Fresh and coked ZSM-5 zeolites

The material used is a hierarchical zeolite resulting from NaOH treatment of a commercial ZSM-5 zeolite with a Si/Al molar ratio of 40. The post-synthesis treatment is already described in ref [18]. Acid and textual properties are summarized in Table 1. The catalyst was coked in a micro-fluidised bed upon pyrolysis of oak at 773 K [19]. The coke content was measured with a SDT Q600 TA thermogravimetric analyser under a 100 mL/min flow of air up to 1173 K. Textural properties were determined by sorption measurements of nitrogen at 77 K, by Micromeritics ASAP 2000 gas adsorption analyzer. Micropore volume was calculated by using the t-plot method. Prior to the measurement, coked samples were outgassed at 363 K for 1 h. The FT-IR measurements were carried out in a Nicolet 750 Magna FTIR 550 spectrometer (resolution 2 cm⁻¹). Samples were shaped in thin disk (20–25 mg) with a diameter of 1.6 cm by using a manual hydraulic press (0.5 ton). The catalyst was activated in situ in the IR cell under secondary vacuum (10⁻⁶ mbar) at 423 K. The concentrations of Brønsted and Lewis acid sites were calculated from the integrated area, after pyridine adsorption at 423 K, of the protonated and coordinated pyridine bands at 1545 and 1450 cm⁻¹, respectively and by using extinction coefficients given in Ref. [20].

2.2. Coke composition

The coke molecules trapped in zeolite pores were recovered after digestion of the spent catalyst using a concentrated hydrofluoric acid solution (51 vol.%). One fraction of coke was soluble in CH₂Cl₂ (soluble coke), the other one insoluble (insoluble coke) led to black particles that can be recovered by a simple filtration, then weighted in order to determine its proportion. The soluble coke fraction obtained after CH₂Cl₂ evaporation was analyzed and quantified by GC-MS (Thermoelectron DSQ) and GC-FID (Agilent), respectively. The soluble and insoluble coke fractions were also characterized by MALDI-TOF MS on a Brüker Autoflex Speed mass spectrometer in a reflectron positive mode where ions were generated by a 337 nm wavelength nitrogen laser. Sample preparations, analysis and calibration methods were done by following the same methodology described in Ref. [21].

2.3. Pin to plate DBD reactor

The reactor used to generate the plasma discharge was a Dielectric Barrier Discharge (DBD) type with a pin to plate geometry (Fig. 1). The disk (20–25 mg, $\phi = 1.6 \text{ cm} \Rightarrow 2 \text{ cm}^2$) is placed directly into the discharge at the surface of the dielectric material (glass).

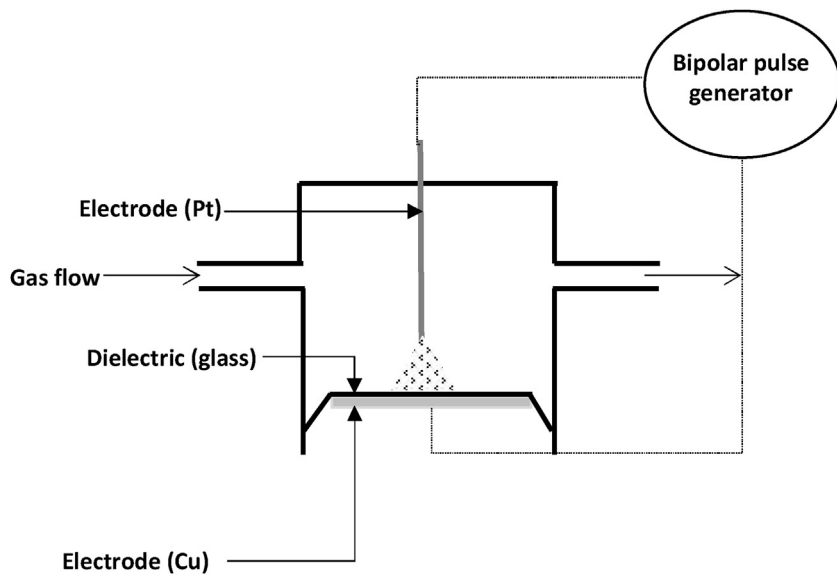


Fig. 1. Scheme of the point to plate DBD reactor.

A high voltage bi-polar pulse generator (A2E technology) was used with a maximum voltage of 40 kV and a variable frequency of up to 8 kHz. The rise time and fall time was 10³ V/ns, the pulse width was 500 ns (Supporting information 1). All experiments were conducted at the same frequency: 2200 Hz while the voltage varied between 9 and 13 kV. The voltage and current measurements were monitored with a digital oscilloscope (Lecroy CT3744, 500 MHz, 46510) through a high voltage probe (Lecroy, PPE 20 kV, 100 MHz) and a current probe (Stangenes Industrie 60 MHz). The deposited power (P) was calculated from the time averaged product of discharge voltage and current. Mass flow regulators (Brooks 5850 TR) control the flow rates. The space velocity through the plasma reactor (GHSV), calculated at ambient temperature and pressure was varied between 300 and 1800 h⁻¹. The gas flow composition after the reactor was analysed with an on-line gas chromatograph (Perkin-Elmer) equipped with a methanizer and a FID detector. A specific analyzer (Environnement SA) was used for ozone quantification.

2.4. Determination of coke removal by the pin to plate DBD reactor

The regeneration of coked zeolite by non-thermal plasma was performed under air or a mixture of He and oxygen. The Gas Hourly Space Velocity (GHSV) was varied from 300 and 1800 h⁻¹, the regeneration time was comprised between 1 and 60 min, and the deposited power was varied from 4 to 16 W. The weight percentage of coke removal was calculated from thermogravimetric analysis, according to the following formula:

$$\eta = \frac{(\text{%coke})_0 - (\text{%coke})_t}{(\text{%coke})_0} \times 100$$

where t corresponds to the regeneration time.

The residual coke content after NTP treatment was measured on the entire disk and also locally at its center.

The concentrations of acid sites were measured at different locations of the disk: at the center, at 3 and 5 mm from the center. The disks were analyzed after plasma treatment using a CMOS camera (8-bit; 2⁸ = 256 Gy levels). The fresh and coked catalysts present respectively a white and black color whereas the treated samples display different shades of gray. The figures of gray levels (GL) were plotted on the integrality of the disks' surface and each point represent the number of pixels in a specific region of interest (ROI)

having the same intensity of gray. For a 8-bit grayscale image there are 256 different shades. The number of pixels on ROI was 434,759 with a magnification of 0.0217 mm/px. The gray level per pixel corresponded to an average value obtained on a square surface of 0.0217 nm per side to the scale disk (1 px = 4.71 10⁻⁴ mm²).

2.5. EPR imaging

2.5.1. EPR image collection

The EPR images were acquired at room temperature using the apparatus: EPR ELEXSYS E580 with two orthogonal water-cooled cylindrical gradient coils using ZY two-axis field gradients. The samples were positioned in the center of an X-band EPR high Q cavity cylindrical resonator (TMS low Q for large sample, 8 mm diameter) operating at 9.5 GHz to minimize the inhomogeneity of the B1 field of the resonator and to allow imaging of the whole wafer. The signals were acquired with a field-of-view of 10 mm and gradient strength of 175 G/cm. The two-dimensional (2D) images were acquired with a size of 512 × 512 pixels resulting in a pixel size of 0.02 mm with a collection of 402 angles in both YZ directions. Microwave power and amplitude modulation were respectively of 2 mW and 2 G. The resolution in the magnetic field direction were 2048 points

2.5.2. EPR image processing

The image processing involves the deconvolution of the whole signal acquired under a magnetic field gradient from the reference signal collected without gradient. Back-projection algorithm using Radon transformation was applied to deconvoluted signal in order rebuild image, giving the spatial distribution of radical species.

The 2D-HYSCORE (hyperfine sublevel correlation) measurements were carried out with the four pulse sequence $\pi/2-\tau-\pi/2-t_1-\pi-t_2-\pi/2-\tau$ echo, and a four-step phase cycle where the echo is measured as a function of t₁ and t₂. The pulse lengths of $\pi/2$ and π pulses in these experiments were 16 and 32 ns, respectively. The 2D-HYSCORE experiments were recorded with a delay τ value of 136 ns that corresponds to the optimum preventing from blind spots effects.

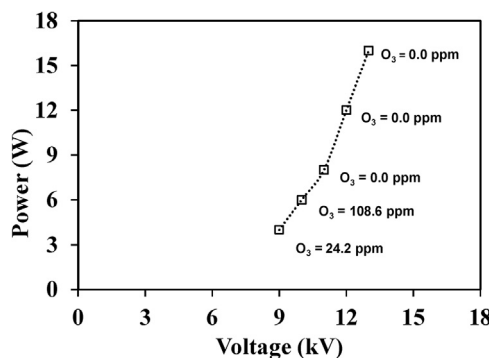


Fig. 2. Deposited power and ozone concentration as a function of input voltage.

3. Results and discussion

3.1. Characterizations of coked zeolite

The amount of coke formed during the catalytic fast pyrolysis of oak on a hierarchical ZSM-5 zeolite, measured by TGA analysis corresponds to 6.5 wt.%. Coke is completely removed under air flow at a temperature higher than 823 K, which corresponds to a typical temperature for the regeneration of this kind of spent catalyst [2]. The residual pore volumes and remaining acid sites are displayed in Table 1. It shows that one part of coke is located within the micropores poisoning Brønsted acid sites. Only micropore volume is affected by coke deposition. The digestion of zeolite framework by hydrofluoric acid followed by a liquid–liquid extraction with methylene chloride leads to two fractions of coke: one soluble (C_{soluble}) in dichloromethane and the other insoluble ($C_{\text{insoluble}}$), with a weight ratio of 2/3. GC–MS analysis indicates that C_{soluble} is mainly composed of alkylbenzenes, alkynaphthalenes. The $C_{\text{insoluble}}$, characterized by MALDI-TOF MS [21], is partly oxygenated due to the origin of the feed (biomass). Its molar weight can be higher than 1000 g/mol (Supporting information 2). The average molar mass of coke (M_{coke}) drawn from its composition is 315 g/mol.

3.2. Non-thermal plasma treatment of coked zeolite

3.2.1. Characterization of the plasma discharge

The coked zeolite was treated under the plasma discharge using an air flow of 100 mL/min. The plasma discharge was characterized according to a classical power versus voltage curve (Fig. 2). The deposited power is an increasing function of the applied voltage. The slope increases above the value corresponding to the breakdown voltage (11 kV), it corresponds to a stable plasma discharge. According to Fig. 2, it was decided to perform experiments with a

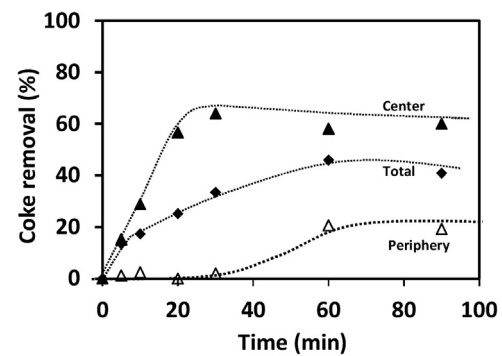


Fig. 4. Coke removal under the plasma discharge as a function of time (Air, $P = 8 \text{ W}$, GHSV = 1200 h⁻¹) on entire (\blacklozenge) and center (\blacktriangle) of the wafer (estimated on its periphery (\triangle)).

deposited power of 8 W. At this power, no ozone was detected due to its low stability under the plasma discharge.

3.2.2. Coke removal efficiency under the plasma discharge

Images of the disk made of coked zeolite, fresh zeolite (without coke) and after plasma treatment (30 min, under 100 mL/min of air, $P = 8 \text{ W}$) are reported in Fig. 3. These images clearly show that the plasma treatment leads to a partial coke elimination since the disk presents a grey color compared to the black color of the coked sample. We checked that the temperature in the plasma zone only slightly increases, the temperature, measured by a laser thermometer, reaches 340 K and stabilized at this value after few minutes (Supporting information 3). Consequently it is possible to state that the coke elimination does not result from a thermal effect but by a direct activation under the plasma discharge. The coke removal was measured locally at the center and the periphery of the wafer and compared with the results obtained for the entire sample. The time of plasma treatment was varied from 5 to 90 min and the results reported in Fig. 4 clearly show that coke is partially removed after only few minutes of plasma treatment (Fig. 4). The weight percentage of coke removed (η), increases with time-on-stream but reaches a plateau at 40%. The coke removal is a local phenomenon, it starts at the center of the disk after only few minutes while coke removal begins after 30 min at the periphery of the wafer. η_{center} increases linearly to reach a plateau at 60 wt.% whereas $\eta_{\text{periphery}}$ is stabilized at 20 wt.%. The results obtained here are not surprising since the electric field is more dense close to the pin electrode, so at the center of the disk, leading to a better efficiency in coke removal.

This difference indicates that the coke removal does not occur by the gas phase but rather by a propagation of active species on catalyst surface. A rough value for the mobility of active species on the catalyst surface can be deduced from the induction period for coke removal in the outer surface of the disk. The propagation rate that includes both coke removal and propagation of the



Fig. 3. Images of the wafer before treatment, fresh catalyst and after plasma treatment (30 min, $P = 8 \text{ W}$, Air GHSV = 1200 h⁻¹).

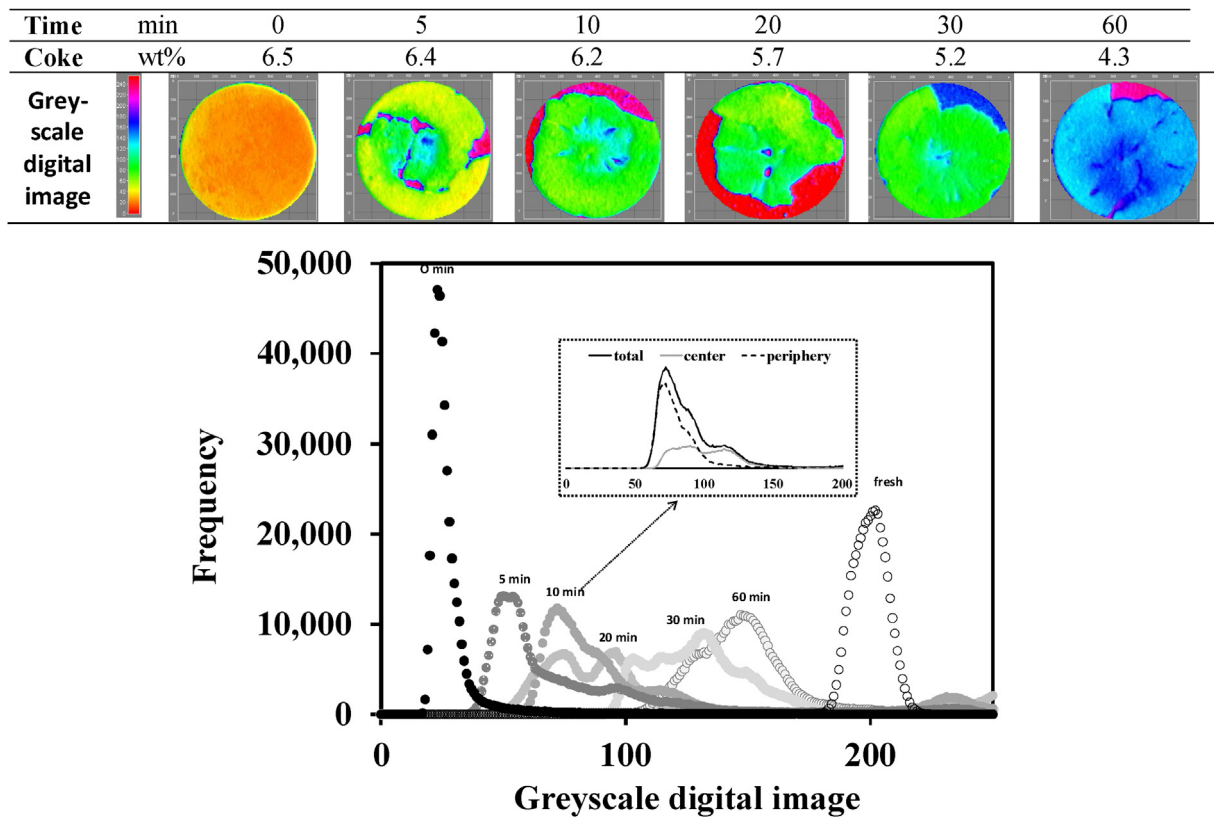


Fig. 5. Greyscale digital image and frequency of grey shades of the disks as a function of time-on-stream (Air, $P = 8\text{ W}$, $\text{GHSV} = 1200\text{ h}^{-1}$).

active species is extremely slow, i.e. 0.8 cm/h . Therefore, the degree of removal depends on the limited diffusion length of the active oxidizing species at the surface.

The color of the disk changes during NTP treatment: initially black it becomes rapidly grey. By using a CMOS camera (Fig. 5), these changes can be “quantified” by measuring the gray level (GL) on the entire disk (GLT) or on different regions of interest: center (GLC) and periphery (GLP). The distribution of GLT is centered to 25 ± 2 for the coked zeolite. On the fresh material, it is slightly broader and centered at 204 ± 3 . Note that on some images, a small part of the disk is broken, leading to the appearance of an artifact at 232. On the partially regenerated catalysts, the GL distributions are obviously between the two previous peaks, but their shapes are much more complex, they can be decomposed into two peaks GLC and GLP more or less overlapped (Fig. 5). After 10 min, only the coke located at the center of the wafer is removed resulting in a broad distribution of GL. No coke at the periphery is removed, but the color changed with a GPL distribution centered at ca 75. This change of color indicates probably a modification in the chemical composition of coke. The amount of coke removal increases with time-on-stream, the disk becomes bright, resulting in an increase of gray level and a narrower width of histograms (i.e. color more homogeneous).

3.2.3. Products formation under the plasma discharge

The analysis of the gas phase was performed on-line at the exit of the reactor. Fig. 6 shows that not only CO_2 is formed but also CO during the plasma treatment. The weight yield of CO_2 and CO are low respectively 12 and 6% on the plateau. From the carbon balance it is possible to conclude that light organic compounds are formed with a weight yield of 22%.

Characterization of the surface of the disk was performed by Infrared spectroscopy in order to observe if coke is transformed

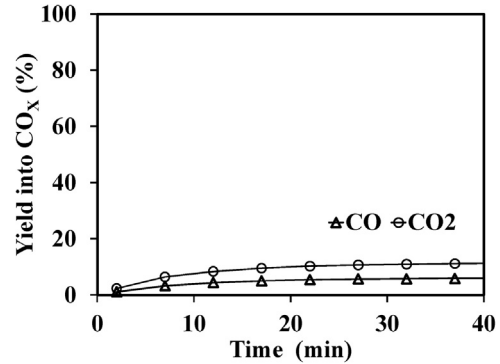


Fig. 6. Weight yields of CO_2 and CO (Air, $P = 8\text{ W}$, $\text{GHSV} = 1200\text{ h}^{-1}$).

during the treatment under plasma. The measurements were performed at three locations of the disk (i.e. 0, 3 and 5 mm from the center) after three treatment times (10, 30 and 60 min). For the coked zeolite, before treatment, Fig. 7 shows the bands characteristic of highly alkylated polycyclic aromatic compounds: 3061 cm^{-1} ($\nu_{\text{as}(-\text{C}-\text{H})}$), 2984 cm^{-1} ($\nu_{\text{as}(\text{CH}_3)\text{ar}}$), 2929 cm^{-1} ($\nu_{\text{as}(\text{CH}_2)\text{ar}}$), 2869 cm^{-1} ($\nu_{\text{s}(\text{CH}_3)}$), 1597 cm^{-1} ($\nu_{\text{as}(\text{C-C})\text{ar}}$), 1507 ($\nu_{\text{s}(\text{C-C})\text{ar}}$) cm^{-1} and 1367 ($\delta_{(\text{CH}_3)}$) [22]. The intensities of the bands are similar regardless of the position on the disk. NTP causes significant changes: the band at 3061 cm^{-1} disappears completely, those at 2974 , 2929 , 2869 and 1367 cm^{-1} decreases, while new bands at 3089 cm^{-1} ($\nu_{\text{as}(\text{CH})\text{ar}}$) and 1751 cm^{-1} ($\nu_{\text{as}(\text{C=O})}$) appear. These changes highlight two oxidation mechanisms: i) the disappearance of the band at 3061 cm^{-1} concomitant with the appearance of a band at 1751 cm^{-1} can be explained by the formation of carboxylic acid from C–H bond and ii) the disappearance of $\nu_{\text{as}(\text{CH}_3)\text{ar}}$ with the appearance of $\nu_{\text{as}(\text{CH})\text{ar}}$ could be due to decarboxylation reaction of benzoic acid.

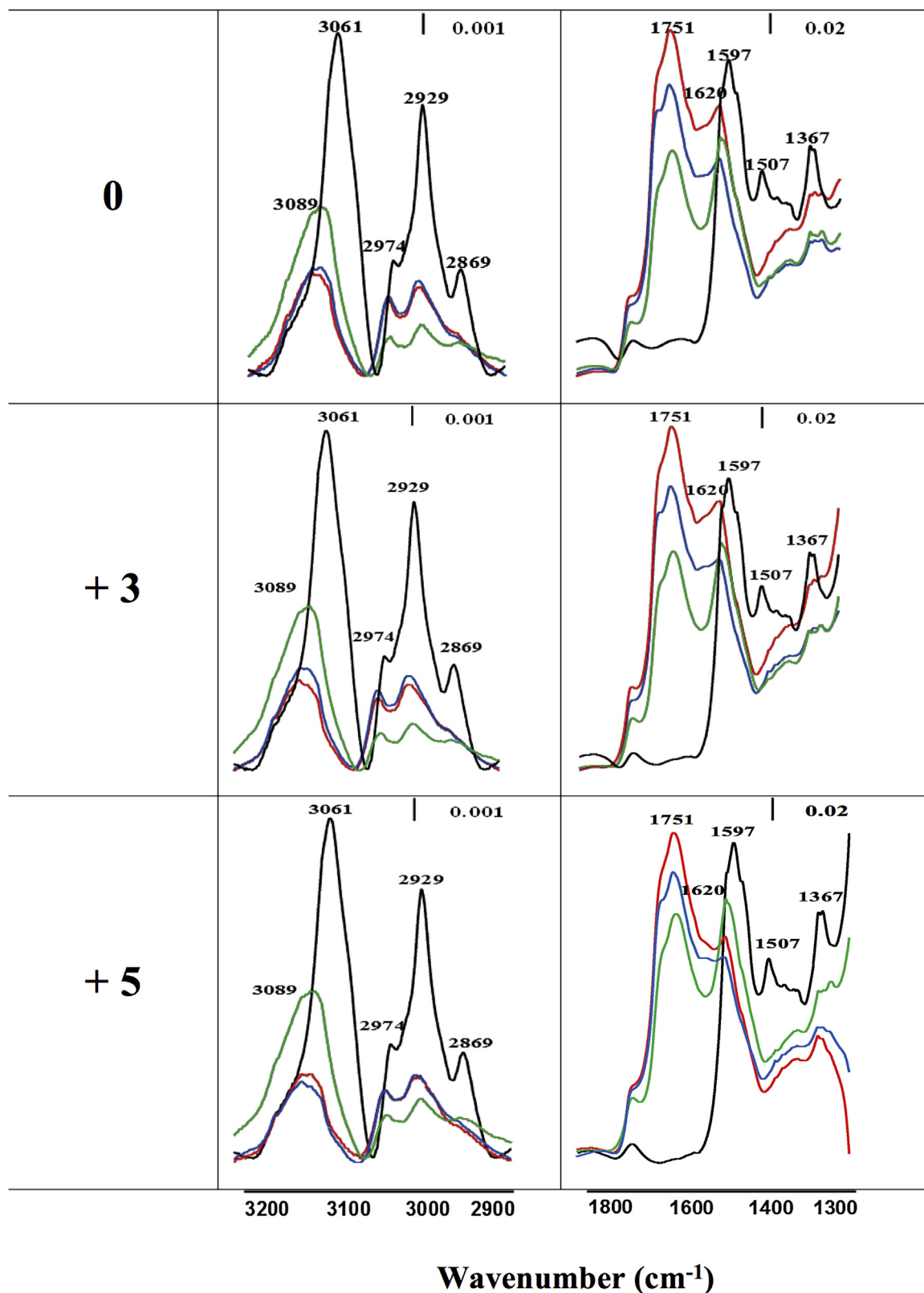


Fig. 7. IR spectra taken in 3 positions on the disk (0, +3, +5): fresh zeolite (black line) and treated catalysts during 10 min (Red) – 30 min (Blue) – 60 min (Green) (Air, $P=8\text{ W}$, $\text{GHSV}=1200\text{ h}^{-1}$). (For interpretation of the references to colour in this figure legend, the reader is referred to the web version of this article.)

The evolution of the concentration of acid sites measured by pyridine at different times and locations is reported in Fig. 8. The BAS concentration is higher after 10 min of treatment under plasma than before treatment. It means that pyridine interacts with other

types of acid sites than BAS, this result can be explained by the presence of carboxylic acid compounds formed by coke oxidation under plasma as revealed by IR analysis. The difference spectra between before and after pyridine adsorption on catalysts displays

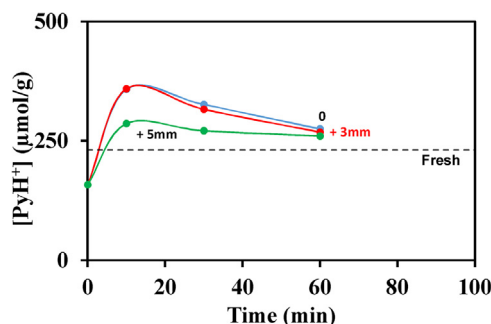


Fig. 8. Concentration of Brønsted acid sites in three positions. 3 and 5 mm from disk's center after regeneration treatment (Air, $P=8\text{ W}$, $\text{GHSV}=1200\text{ h}^{-1}$).

a negative band at 1751 cm^{-1} , confirming that the basic probe neutralized carboxylic acids (Supporting information 4). From M_{coke} (315 g/mol), η (Fig. 4) and the number of pyridinium ions (Fig. 8), it is possible to estimate a rough proportion of oxidized coke molecules presents on the spent catalyst as functions of both treatment time and location on the disk (Supporting information 5). The average number of carboxyl group per molecule of coke in the center of the disk is initially ca 1, then it decreases with TOS. At the periphery of the disk, it is only 0.3, regardless of the regeneration time. The formation of carboxylic groups leads to the brightening of the disk (increase of the grey scale, Fig. 5).

3.2.4. Spatial characterization of coke by 2D-EPR spectroscopy

Coke molecules trapped within the zeolite can lead by spontaneous ionization to the formation of radical species that can be located spatially on the sample by using EPR [17]. Previous works revealed the presence of radical species on coke molecules [16]. These species can be used as probe to check if plasma treatment is able to access and diffuse inside the zeolite micropores. 2D-EPR images obtained on the disks at different treatment times are summarized in Fig. 9.

EPR images are superimposed on disk's picture to show directly the spin density distribution within the sample. Note that the disks have been placed in a random manner on the sample holder. These images display a color bar giving the spatial spin concentration distribution with the two extremum purple and red colors that display respectively the region with no paramagnetic species and highest concentration, in radical content. Green and blue colors indicate zones of medium (50%) and low (25%) spin concentrations, respectively. Initially, we observe that spin density distribution is quite homogeneous on the disk but changes quickly appear. A drastic color change appears after the non-thermal plasma treatment with a prominent greenish zone after 5 min while a bluish zone is dominant after 60 min of treatment, revealing a heterogeneous distribution of spin density on the disk. Indeed, one can observe that spin density is concentrated in a specific zone on the disk's periphery which is more marked with prolonged treatment time. The plasma treatment involves a center poor zone in spin density while the periphery of the disk is a rich zone in spins. These observations corroborate previous results obtained by greyscale digital image and with the percentage of removal coke which start on the disk's center. As radical species are localized on coke molecules, we can estimate the percentage of radical coke removal by using the quantification of these species by continuous wave EPR. The local concentration of radical species is summarized in Table 2.

The CW-EPR spectra exhibits an intense lorentzian line with a g factor of 2.0034 (not shown here). The quantification shows a fast drop of 70% in radical concentration between 5 min and 20 min and then an increase of approximately 50% in radical concentration after 30 min (Table 2). This raise is probably due to radical species

Table 2
Radical concentration by using CW-EPR spectroscopy.

Time (min)	[Spin] ($\mu\text{mol/g}$)	$\Delta\text{H: Linewidth (G)}$
5	0.35	5.98
20	0.11	5.66
30	0.24	5.43
60	0.31	5.60

generated by plasma. Indeed, from 5 min of plasma treatment, a second contribution is observed on CW-EPR spectrum corresponding to a radical species which are probably formed by the plasma. Indeed, we observed that the lineshape of EPR spectrum is very well fitting by one contribution for coked sample which means the presence of radical species with similar nature. However, this is not the case for samples after plasma treatment (5 min and 60 min) with a detection of a second contribution which means the presence of a second radical species (Supporting information 6). One can assume that initially the radical species are carbon center radical and after plasma treatment a second species is formed which is probably characteristic of oxygen center radical. So, the active species generated by the plasma are able to diffuse within the zeolite micropores which have never been reported up to date. During the plasma treatment, the linewidth of the CW-EPR spectra decreases due to a dehydrogenation of coke molecules (Table 2). This phenomenon is corroborated by HYSCORE (HYperfine Sublevel CORrelation) sequence by using pulsed EPR. HYSCORE are recorded at two τ values (136 and 200 ns) to avoid blindspot phenomenon. The signal intensity ratio $^{13}\text{C}/^1\text{H}$ calculated with the two τ values, is clearly larger after 60 min than after 5 min which may be related to the high aliphatic branching of aromatic units (Fig. 9). These differences in $^{13}\text{C}/^1\text{H}$ ratio may also reflect size differences of aromatic fragments which means that aromatic radicals of coke molecules are larger after 60 min than those after 5 min. In conclusion, the EPR spectroscopy (Continuous Wave, Imaging and pulsed techniques) highlighted that plasma treatment involves a distribution change of radical coke more concentrated on the disk's periphery accompanied with the formation of new family of coke molecules: initially carbon centered radicals towards probably oxygen centered radicals with a high aliphatic branching of aromatic units.

3.3. How to improve the efficiency of NTP regeneration treatment?

3.3.1. Influence of GHSV and deposited power

The influence of GHSV and deposited power on carbon removal were examined, the results obtained after 30 min of plasma treatment are reported in Fig. 10.

η depends on both deposited power (P) and gas hourly space velocity (GHSV) (Fig. 10). With an instable plasma ($P < 8\text{ W}$) the percentage of removed coke is low (<25 wt.%), in spite of the presence of a large amount of O_3 (Fig. 2), η decreases very slightly with GHSV. The change of color indicates some modifications on the chemical coke composition, probably the formation of acid carboxylic groups. With a stabilized NTP ($P \geq 8\text{ W}$), η increases with the deposited power but the gain is not proportional to P . The increase of GHSV improves surprisingly η (Fig. 10). The gray level images show that a high flow rate favours the propagation of the active species generated by the plasma on the surface of the disk and maybe within the zeolite micropores. The benefit effect of an increase of the flow rate on coke removal could be related to an extension of the ionic wind, hence of the diffusion length of the oxygenated active species on the disk [23].

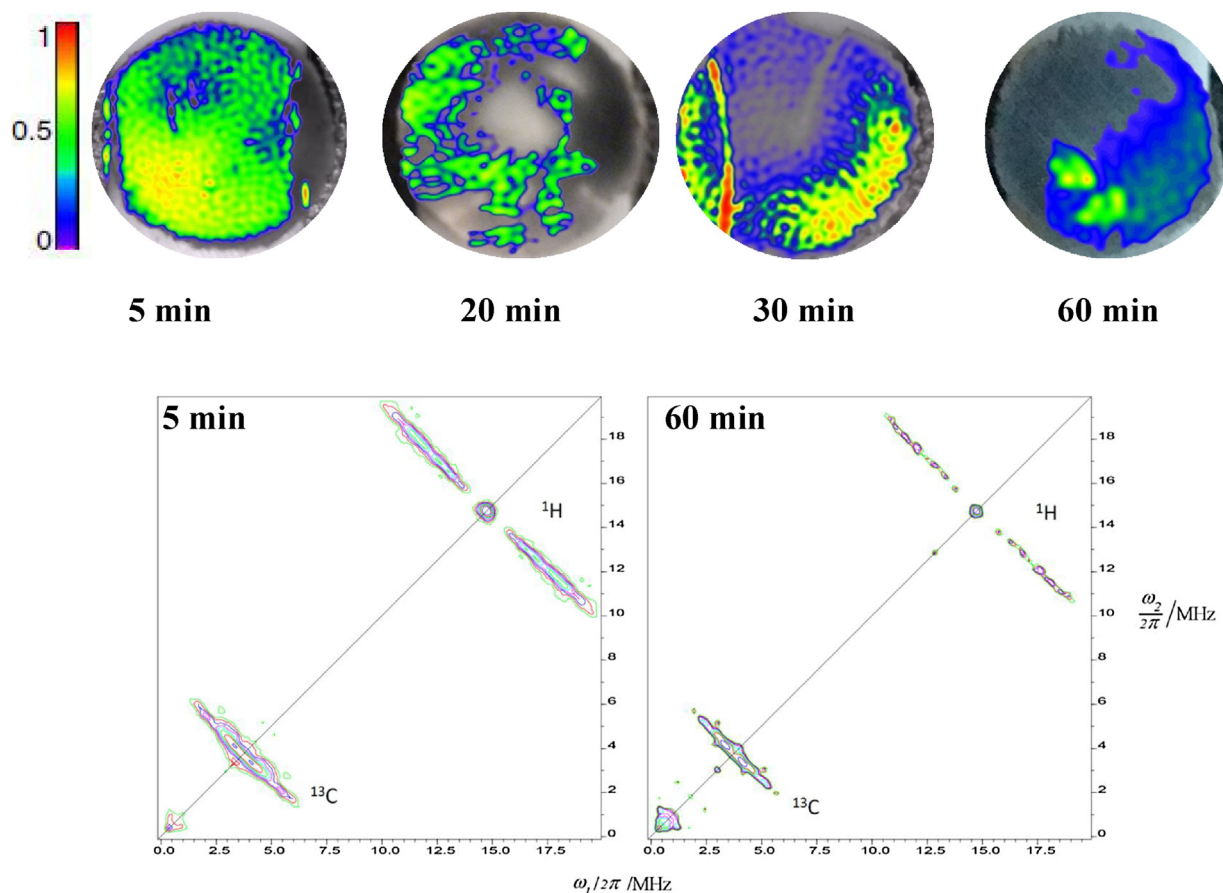


Fig. 9. 2D-EPR images of spin density distribution on the disk ($\phi = 9$ mm) and 2D-HYSCORE spectra as a function of time treatment. (Air, $P = 8$ W, GHSV = 1200 h^{-1}).

Table 3

Properties of regenerated ZSM-5 zeolite by using a non-thermal plasma (mixture He-O₂: 80/20, $P = 8$ W, GHSV = 1200 h^{-1}).

Coke ^a (wt.%)	$V_{\text{micro}}^{\text{b}}$ (cm ³ /g)	$V_{\text{meso}}^{\text{c}}$ (cm ³ /g)	[PyH ⁺] ^d (μmol/g)	[PyL] ^e (μmol/g)
0	0.13	0.40	247	64

^aMeasured by ATD/ATG; ^bmicropore volume obtained by using t-plot method; ^c mesopore volume = $V_{\text{total}} - V_{\text{micro}}$ (V_{total} determined from the adsorbed volume at $p/p_0 = 0.99$); ^{d,e} measured by pyridine adsorbed on Brønsted and Lewis acid sites after evacuation at 423 K.

3.3.2. Influence of the nature of gas

The plasma treatment was performed using a mixture of helium and oxygen instead of nitrogen and oxygen. The deposited power was maintained at 8 W by decreasing the applied voltage (U) from 11 to 9.1 kV. After 30 min of treatment the recovered disk presents a homogeneous white colour and the weight yield of coke elimination is higher than 95%. All the poisoned Brønsted acid sites as well as initial textural properties are recovered after only 20 min of treatment (Table 3). The coke combustion is 6 times faster than with air and furthermore is almost totally selective in CO₂ (Fig. 11) (more than 95% of carbon atoms are in CO₂). This total oxidation confirms that under air one part of coke was transformed into light organic molecules.

The active species responsible for coke removal are oxygen species since with helium only at 8 W (U = 9.1 kV) the efficiency is limited to 20%; the activated He species are able to remove, probably by cracking reactions, some coke molecules. Secondly, we checked that He enriched with ozone (>0.2 vol.%) is unable to remove coke at room temperature. A complete oxidation by ozone requires a moderate thermal activation. Indeed, Fan et al. [24] have shown that a coked zeolite by biomass pyrolysis vapors can be totally regenerated using ozone at 623 K. The decoking process is believed to depend on the density of O atoms generated

by the plasma discharge [25]. The role of the noble gas (He) is to enhance the efficiency of production of active O atoms manifolds according to Khan et al. [26] and Moselhy et al. [27]. Indeed helium presents a much more energetic Electron Energy Distribution Function (EEDF) than nitrogen, which leads to a higher ionization coefficient and consequently a higher O atoms yield [28]. Collisions of energetic electrons with helium leads to the formation of species in metastable state: $e + He \rightarrow He^* + e$. An energy transfer from excited He to O₂ molecules proceeds resulting in dissociation through the formation of O₂⁺ ions yielding O atoms: $He^* + O_2 \rightarrow O_2^+ + e + He$ and $O_2^+ + e \rightarrow O^+ + O^-$.

It seems very unlikely that a plasma discharge penetrates the micropores of a ZSM-5 zeolite ($\phi = 5.1 \times 5.5 \leftrightarrow 5.3 \times 5.6$), or that activated species are still present after few collisions with the channels of the medium pore zeolite. But the results obtained in the present study prove that oxygenated species produced under non-thermal plasma are able to access the porosity of the zeolite removing completely coke even those located into micropores. To explain this results two hypothesis can be drawn: 1) the formation of microdischarges inside the catalyst pores, 2) the migration of active oxygen species from the gas bulk into the pores. The formation of microdischarges inside catalyst pores was reported by some authors [29,30]. Zhang et al. [31] in a modeling investigation,

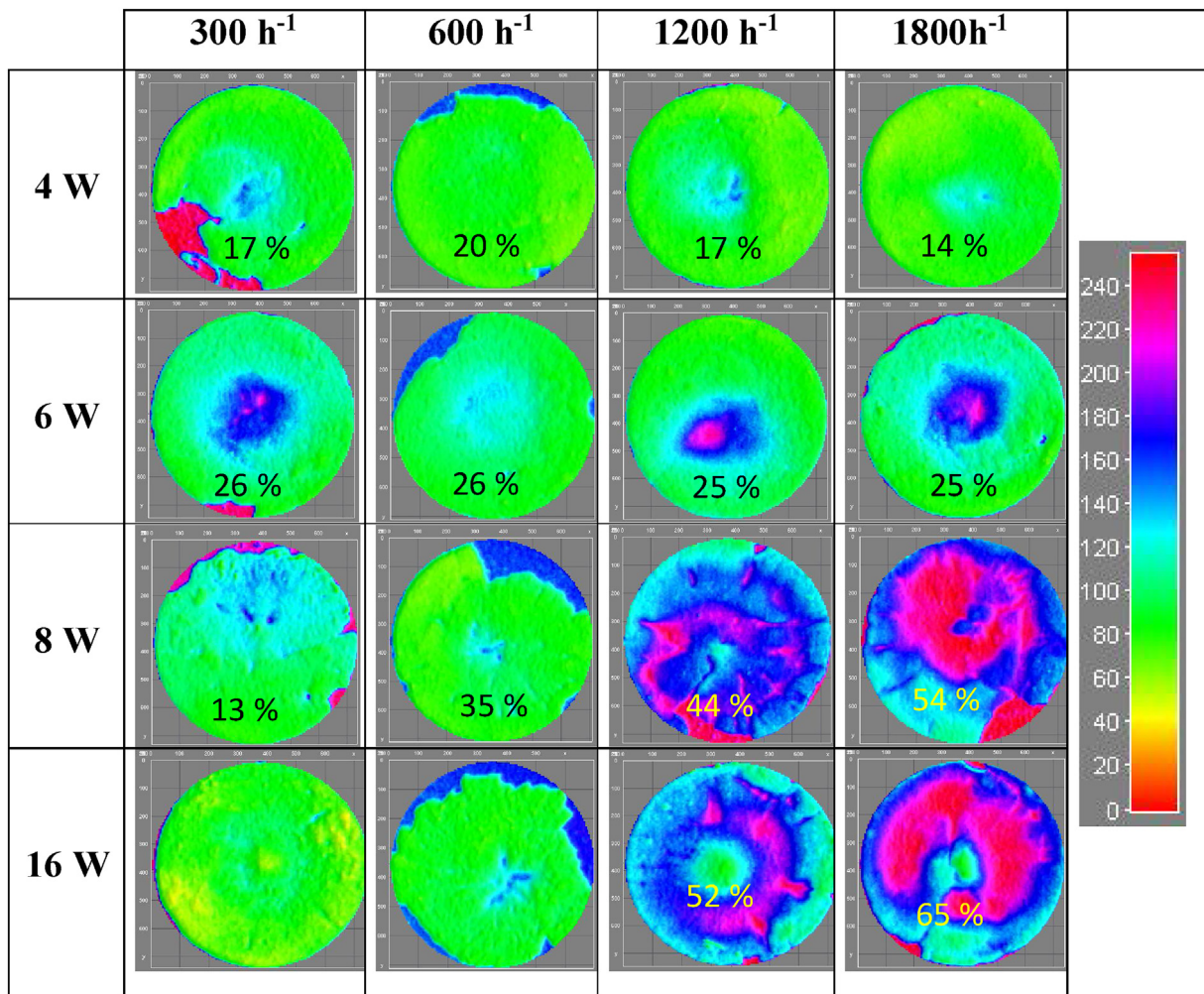


Fig. 10. Grayscale digital image of the disks and yield into coke removal as a function of gas hourly space velocity for 4, 6, 8 and 16 W generated power. (Air, t = 30 min).

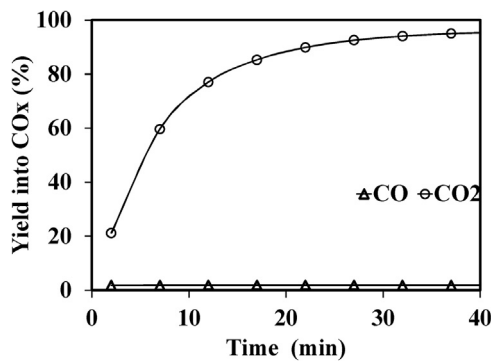


Fig. 11. Weight yields of CO_x as a function of time: (mixture He-O₂: 80–20%), P = 8 W, GHSV = 1200 h⁻¹).

showed that plasma can be formed inside pores of structured catalysts in a micrometer range. It is believed that microdischarges cannot be formed into sub- μm pores because the electric field is not enough strong in the porosity. However the calculations were performed in glow mode characterized by low electron density, which differ strongly from the plasma used in the present work.

The pulsed high-voltage power used in the present study allows the development of fine discharge channels. In this case the charge emitted from the pin electrode is accumulated on the dielectric layer and intensifies the electric field in the zone where the coked

zeolite is localized. Consequently the formation of microdischarges into the zeolite porosity can be proposed.

The migration of short-lived species from the gas phase into the pores was proposed by Holzer et al. [32]. The authors showed that atomic oxygen species O⁺ are chemisorbed at the surface of the catalyst. The species would be stabilized by adsorption leading to a significant increase of the lifetime of reactive species. Under our experimental conditions the combination of the two explanations can be proposed: activated oxygen species would be formed into the mesoporosity of the zeolite, the active species penetrate the micropores by diffusion and migration leading to coke removal. The radical species associated with coke, evidenced by EPR, and localized into the microporosity of the zeolite could also contribute to the mechanism of coke removal by charge transfer. The zeolite is an ionic media favoring the stabilization and diffusion of ionic and radical species.

4. Conclusion

The regeneration of a coked HZSM5 zeolite was investigated using a DBD plasma reactor. We show in this study that a pin to plate geometry was effective to remove coke at room temperature with a deposited power as low as 8 W. The coke localized at the centre of the catalyst, shaped as a wafer, is eliminated first due to the intense electric field localized close to the pin electrode. The periphery of the disk is affected by the plasma treatment after a delay of 30 min

under air and a gas flow rate of 100 mL/min. Analysis by grey level clearly show the heterogeneity of coke localization after plasma treatment and the evolution of coke elimination with time of treatment. Coke is removed as CO₂ and CO, but also as light organic compounds. IR analysis show that coke is also partially oxidised into carboxylic acid under the plasma discharge using air. 2D-EPR images obtained on the disks at different treatment time exhibit the presence of a different type of radical species which are probably formed by the plasma. It is believed that the radical species are initially carbon center radical and after plasma treatment a second type of species is formed which is probably characteristic of oxygen center radical. So, according to the localization of the radical species, it is proposed that the active species generated by the plasma are able to diffuse within the zeolite micropores which has never been reported up to date.

An almost complete zeolite regeneration was possible by substituting nitrogen in the feed gas by helium. In this case coke is oxidized selectively into CO₂, six time faster than under air.

Acknowledgement

We thank CNRS's infrastructure RENARD (FR3443) for EPR facilities.

Appendix A. Supplementary data

Supplementary data associated with this article can be found, in the online version, at <http://dx.doi.org/10.1016/j.apcatb.2017.07.040>.

References

- [1] C.H. Bartholomew, M.D. Argyle, Advances in catalyst deactivation and regeneration, *Catalysts* 5 (2015) 949–954.
- [2] M. Guisnet, Regeneration of coked zeolite catalysts, in: M. Guisnet, F. Ramôa Ribeiro (Eds.), *Deactivation and Regeneration of Zeolite Catalysts*, Imperial College Press, London, 2011, pp. 217–231.
- [3] C.H. Bartholomew, *Appl. Catal. A. Gen.* 212 (2001) 17–60.
- [4] M. Guisnet, Mode of coke formation and deactivation, in: M. Guisnet, F. Ramôa Ribeiro (Eds.), *Deactivation and Regeneration of Zeolite Catalysts*, Imperial College Press, London, 2011, pp. 115–137.
- [5] M. Guisnet, P. Magnoux, *Catal. Today* 36 (1997) 477–483.
- [6] K. Moljord, P. Magnoux, M. Guisnet, *Appl. Catal. A Gen.* 121 (1995) 245–259.
- [7] J. Biswas, I.E. Maxwell, *Appl. Catal.* 63 (1990) 197–258.
- [8] G.J. Hutching, R.G. Copperthwaite, T. Themistocleous, G.A. Foulds, A.S. Bielovitch, B.J. Loots, G. Nowitz, P. van Eck, *Appl. Catal.* 34 (1987) 153–161.
- [9] O. Sanchez-Galofré, Y. Segura, Y. Pérez-Ramírez, *J. Catal.* 249 (2007) 123–133.
- [10] B. Eliasson, C.J. Liu, U. Kogelschatz, *Eng. Chem. Res.* 39 (2000) 1221–1227.
- [11] X. Tu, B. Verheyde, S. Corthals, S. Paulussen, B.F. Sels, *Phys. Plasmas* 18 (2011) 80702–80710.
- [12] B. Eliasson, U. Kogelschatz, *IEEE Trans. Plasma Sci.* 19 (1991) 309–323.
- [13] D.M. Bibby, N.B. Milestone, J.E. Patterson, P. Aldridge, *J. Catal.* 97 (1986) 493–502.
- [14] M.A. Khan, A.A. Al-Jalal, *Appl. Catal. A: Gen.* 272 (2004) 141–149.
- [15] N. Hafezkhiaabani, S. Fathi, B. Shokri, S.I. Hosseini, *Appl. Catal. A: Gen.* 493 (2015) 8–16.
- [16] K. Ben Tayeb, K. Pinard, L. Touati, N. Vezin, H. Maury, S. Delpoux, *Catal. Commun.* 27 (2012) 119–123.
- [17] M. Sathiya, J.-B. Leriche, E. Salager, D. Gourier, J.-M. Tarascon, H. Vezin, *Nat. Commun.* 6 (2015) 1–7.
- [18] C. Fernandez, I. Stan, J.-P. Gilson, K. Thomas, A. Vicente, A. Bonilla, J. Pérez-Ramírez, *Chem. Eur. J.* 16 (2010) 6224–6233.
- [19] L. Jia, Y. Le Brech, B. Shrestha, M. Bente von Frowein, S. Ehler, G. Mauviel, R. Zimmermann, A. Dufour, *Energy Fuels* 29 (2015) 7364–7374.
- [20] M. Guisnet, P. Ayrault, J. Datka, *Pol. J. Chem.* 71 (1997) 1455.
- [21] L. Pinard, S. Hamieh, C. Canaff, F. Ferreira Madeira, I. Batonneau-Gener, S. Maury, O. Delpoux, K. Ben Tayeb, Y. Pouilloux, H. Vezin, *J. Catal.* 299 (2013) 284–297.
- [22] H.S. Cerqueira, P. Ayrault, J. Datka, M. Guisnet, *Microporous Mesoporous Mater.* 38 (2000) 197–205.
- [23] N. Benard, P. Note, M. Caron, E. Moreau, *J. Electrostat.* 88 (2017) 41–48.
- [24] M.A. Khan, A.M. Al-Jalal, *J. Appl. Phys.* 104 (2008) 123302–123310.
- [25] Y. Fan, Y. Cai, X. Li, H. Yin, L. Chen, S. Liu, *J. Anal. Appl. Pyrol.* 11 (2015) 209–215.
- [26] A.M. Al-Jalal, M.A. Khan, *Plasma Chem. Plasma Process.* 30 (2010) 173–182.
- [27] M. Moseley, R.H. Stark, K.H. Schonenbach, U. Kogelschatz, *Appl. Phys. Lett.* 78 (2001) 880–884.
- [28] P. Viegas, A. Bourdon, L.L. Alves, V. Guerra, 42nd EPS Conference on Plasma Physics (2015) 305.
- [29] U. Roland, F. Holzer, F.D. Kopinke, *Appl. Catal. B: Environ.* 58 (2005) 217–226.
- [30] K. Hensel, S. Katsura, A. Mizuno, *IEEE Trans. Plasma Sci.* 33 (2005) 574–575.
- [31] Y.R. Zhang, K. Van Laer, E.C. Neyts, A. Bogaerts, *Appl. Catal. B: Environ.* 185 (2016) 56–67.
- [32] F. Holzer, U. Roland, F.D. Kopinke, *Appl. Catal. B: Environ.* 38 (2002) 163–181.